Hindawi
Geofluids
Volume 2021, Article ID 3401273, 17 pages
https://doi.org/10.1155/2021/3401273

Research Article

Multiple Influences of Paleogeography, Sequence Stratigraphy, and Fold Structure on Coalbed Methane Accumulation in the Lopingian (Late Permian) of Junlian Coalfield, SW China

Xiangdong Gao,[1,2] **Wuzhong Li**,[3] **Yiming Yang**,[4] **Kaigui Yin**,[5] **and Shihao Zhou**[1]

[1]*School of Earth Science, East China University of Technology, Nanchang, Jiangxi 330013, China*
[2]*State Key Laboratory of Oil and Gas Reservoir Geology and Exploitation, Chengdu University of Technology, Chengdu 610059, China*
[3]*PetroChina Research Institute of Petroleum Exploration & Development, Beijing 100083, China*
[4]*Research Institute of Petroleum Exploration and Development, PetroChina Liaohe Oilfield Company, Panjin, Liaoning 124010, China*
[5]*PetroChina Zhejiang Oilfield Company, Hangzhou, Zhejiang 310023, China*

Correspondence should be addressed to Wuzhong Li; lwzmcq69@petrochina.com.cn

Received 9 July 2021; Revised 28 August 2021; Accepted 13 September 2021; Published 14 October 2021

Academic Editor: Xudong Zhang

Junlian coalfield is one of the main targets for coalbed methane (CBM) exploration and development in the southwest China. Based on field geological survey, core observation, gas content statistics, coal maceral composition, vitrinite reflectance (R_O), proximate analysis and trace element test, lithological types, lithofacies, sedimentary environment, and structural analysis, this research established the sequence stratigraphy frame, revealed the plane distribution characteristics of sedimentary facies, and defined CBM accumulation mode. The results show that six rock types were identified and further subdivided into twenty lithofacies types. Four types of sedimentary systems such as alluvial plains, delta, lagoon-tidal flat, and carbonate platform were summarized according to their combination characteristics. Additionally, 12-14 fourth-order sequences and three third-order sequences CSI, CSII, and CSIII were divided, and a sequence stratigraphic framework of the Lopingian coal-bearing series was established. Among them, the features of third-order sequence CSIII paleogeography from west to east are alluvial plains, deltas, lagoon-tidal flats, and limited carbonate platforms. Thick coal seams are mainly developed in the sedimentary environment of tidal flats, delta plains, and floodplains behind banks. Closely related to coal seam thickness, gas contents of Lopingian coal seams are generally higher than 8 m^3/t, except the low level in northwest and partial denudation areas. CBM accumulation is significantly controlled by the fold structure, and the hydraulic plugging effect makes the syncline core favorable for CBM accumulation. Furthermore, favorable geostress conditions enable the secondary anticline to become a favorable area for CBM accumulation when the sealing conditions are better. This research will provide a theoretical guide for the exploration and development of CBM in the study area.

1. Introduction

During the past 20 years, CBM has emerged as an important energy resource and is expected to be a significant component in the future world energy portfolio. CBM is considered a clean fuel because its combustion releases no toxins and ash and less carbon dioxide per unit of energy than the combustion of coal, oil, or wood [1, 2]. These advantages, as well as rapidly growing worldwide energy demands, are prompting many countries having large coal resources to evaluate the CBM potential of coal basins [3, 4]. China is rich in CBM resources, and the economic production of CBM has been successfully achieved from shallow coal seams [5, 6]. However, the CBM development activities in China have

an extremely uneven geographical distribution concentrated in North China, especially in the southern Qinshui Basin and eastern Ordos Basin [7, 8]. Southern Sichuan is an important coal-producing region in South China. With a high degree of coal thermal evolution and a wide development area, the CBM resources are abundant in the Lopingian coal-bearing rock system [9]. Junlian coalfield is an important target area for CBM exploration and development in this area [10]. Nevertheless, the CBM exploration and development have not reached commercial breakthroughs. One of the main reasons is the lack of understanding of the CBM accumulation under the complex geological conditions in the study area.

Many scholars have conducted in-depth research on CBM geology in southern Sichuan [11, 12]. They have realized that the resource potential of CBM is affected by the thickness of the coalbed, buried depth, gas content, coal and rock composition, roof and floor lithology and hydrodynamic conditions, and other factors. The depositional environment of coal-bearing rock series controls the development of coal seams, which in turn affects the generation, storage, and preservation conditions of CBM, and directly affects the level of CBM content [13]. Structure is an important controlling factor for the evolution of coal reservoirs and the adjustment of the occurrence of CBM, and it is also a key factor affecting the current gas content of coal reservoirs [14]. At present, some scholars tend to agree that the CBM enrichment areas are mainly located in coal-accumulating structural units dominated by synclines [15, 16]. Therefore, it is very necessary to clarify the depositional environment of coal accumulation period and current structural features of coal reservoirs.

Based on field geological survey, core observation, gas content statistics, coal maceral composition, vitrinite reflectance (R_O), proximate analysis and trace element test, lithological types, lithofacies, sedimentary environment, and structural analysis, this study is aimed at building the sequence stratigraphy frame, clarifying the sedimentary environment of coal formation period, revealing distribution characteristics of gas content in coal reservoirs, deepening CBM accumulation mode, and providing a theoretical guide for the exploration and development of CBM in the study area.

2. Geological Background

The Junlian coalfield, located in the south of Sichuan Province, is an important part of the southern Sichuan coalfield and one of the main targets of CBM exploration and development in the southwest China (Figure 1(a)) [10]. In the Late Permian, it was located at the southwest margin of the Upper Yangzi Craton Basin tectonically, which is part of the intact South China Plate, and the Lopingian coal-bearing series was developed on a stable sedimentary basement [17, 18]. After the Lopingian deposition, Junlian area experienced superposition of multiple phases of tectonic movements, forming a pattern of alternate distribution of multiple obliques and back slopes (Figure 1(b)) [19]. The coal seams are mainly located inside these obliques or on the two flanks of the back slope, with the dip angle of the coal seams larger at the edge of the oblique and gentler at the core of the oblique. The coal seams are mostly exposed or stripped at the edge of the oblique and back slope, and the burial depth of the main coal seams is generally less than 2000 m. Coal types range from fat, coking, lean, poor to anthracite and are mainly high-rank bituminous coals and low-rank anthracite coals [10], with the maximum vitrinite reflectance between 0.67% and 3.49% and the volatile fraction yield generally less than 10%. The coal rock types dominate semidark to semibright with strong luster. Mirror coal and bright coal show diamond luster, in black, gray-black, or lead gray color and mostly with linear or fine to medium stripes and few flake structure [20].

The Longtan Formation and Changxing Formation are the main coal-bearing series in the Lopingian. The Longtan Formation was mainly formed in a sea-land transitional environment with a stratigraphic thickness of 50-130 m mainly consisting of conglomerate, sandstone, mudstone, coal, and limestone. The bottom is usually unconformably overlain on the basal Emeishan basalt or the tuff of the Maokou Formation, and the top was in integrated contact with the Changxing Formation [21, 22]. There are about 1~30 coal layers developed in the Longtan Formation, and the main mineable coal seams are C_2, C_3, C_7, and C_8. The Changxing Formation dominantly comprises marine carbonate rocks and sea-land transitional deposits, including limestone, mudstone, coal seam, and fine sandstone, with stratigraphic thickness of 40-80 m and No. 0-10 coal seams [23] as well as abundant paleontological fossils including plants, brachiopods, petrous gills, foraminifera, Fusulinida, moss worms, and coral species, specifically *Gigantopteris dictyophylloides Gu and Zhi*, *Lepidodendron acutangulum*, *G. nicotianaefolia*, *Lobatannularia heianensis*, *Plagiozamites oblongifolius*, *Phricodothyris asiatica*, *Oldhamina squamosa*, and *Aviculopecten* sp., etc. [24]. The top layer was in integrated contact with the Lower Triassic Feixianguan Formation.

3. Methods

The enrichment of CBM is mainly dependent on the development characteristics of coal seams, which are inextricably linked to the depositional environment [25, 26]. Petrographic paleogeographic analysis can reconstruct the geological landscape and environment based on the petrographic features [27], and the petrographic parameters can independently reflect the characteristics of the depositional environment in a particular geological period [17].

This research established a database for analyzing coal accumulation and CBM enrichment law. The data consists of 39 boreholes and outcrop profiles covering the entire study area. Paleogeographic parameters such as stratum thickness, sandstone thickness, mudstone thickness, limestone percentage, coal seam percentage, and the ratio of sand to mud were analyzed. The lithofacies paleogeography was reconstructed by the single-factor analysis and multiple-factor comparison method. Additionally, coal seam thickness, coal maceral content, ash yield, and sulfur content, as well as 30 gas content

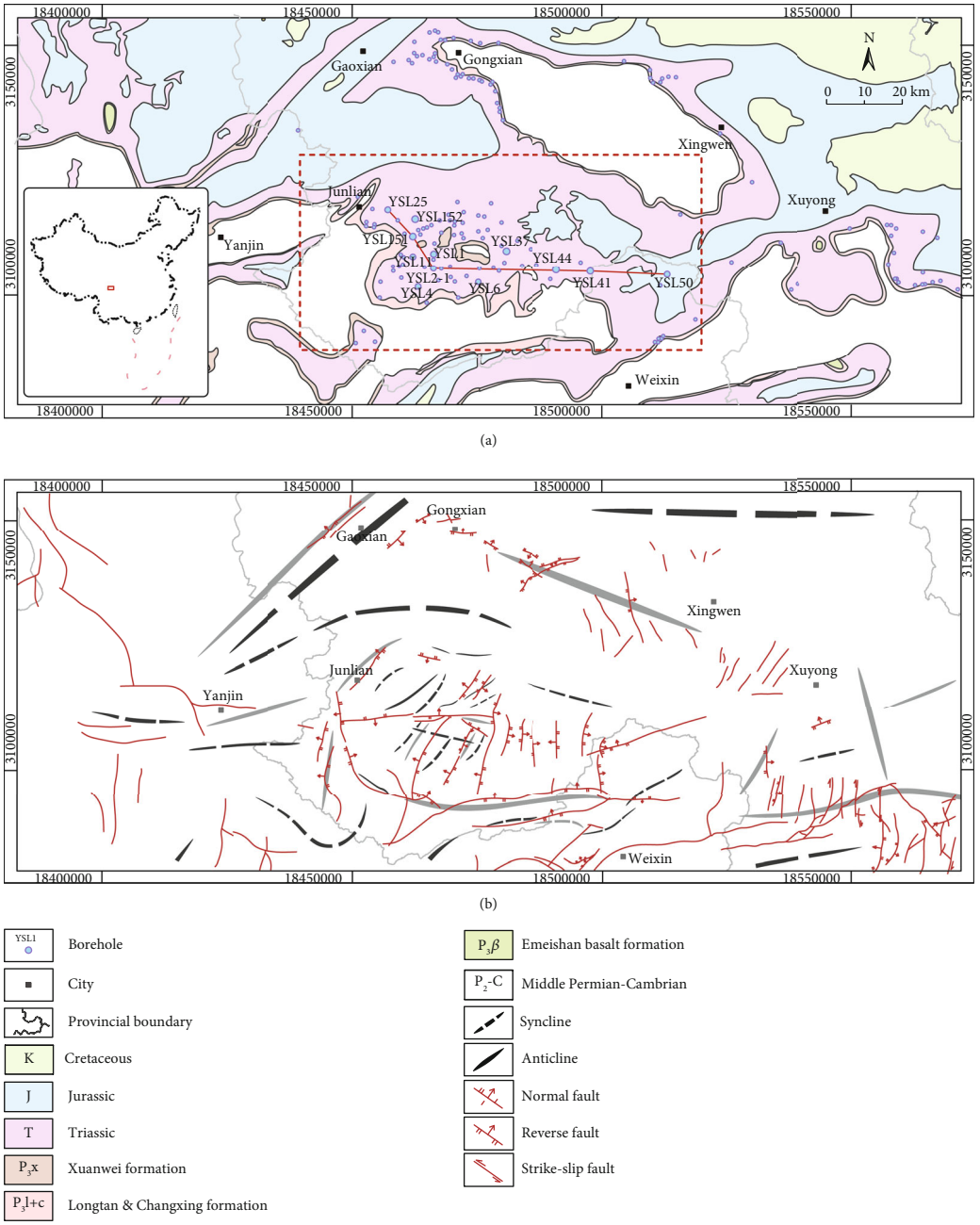

Figure 1: Stratigraphic distribution and tectonic outline of the Junlian coalfield.

data of $C_2 + C_3$ coal seam in Changxing Formation and 39 gas content of $C_7 + C_8$ coal seam in Longtan Formation, were calculated. R_O measurement and coal maceral composition identification were both implemented with a Leitz MPV-3 photometer microscope. The R_O measurement followed the China National Standards GB/T 6948-1998. Coal maceral composition identification followed the China National Standards GB/T 8899-1998. The proximate analysis, which was used to obtain ash content, moisture, and volatile content of the coal, was performed following the China National Standards GB/T212-2008. Trace elements were analyzed by plasma mass spectrometer ICP-MS, with a test temperature of 23.6°C and a relative humidity of 41.9%. In the analysis, the sample was dissolved in a closed sample dissolver with hydrofluoric acid and nitric acid, and the hydrofluoric acid was evaporated on an electric heating plate; then the samples were sealed and dissolved with nitric acid. After dilution, the content of elements was determined by ICP-MS external standard method. Finally, the calculation and correction are carried out, and the error is less than 5%.

The sequential process to study the influence of coal forming environment on methane accumulation in the Lopingian coal seams of Late Permian in Junlian area is as follows: (1) clarify the controlling effects of sedimentary environment on the thickness distribution of coal seam, coal maceral content changes, and ash and sulfur content as well

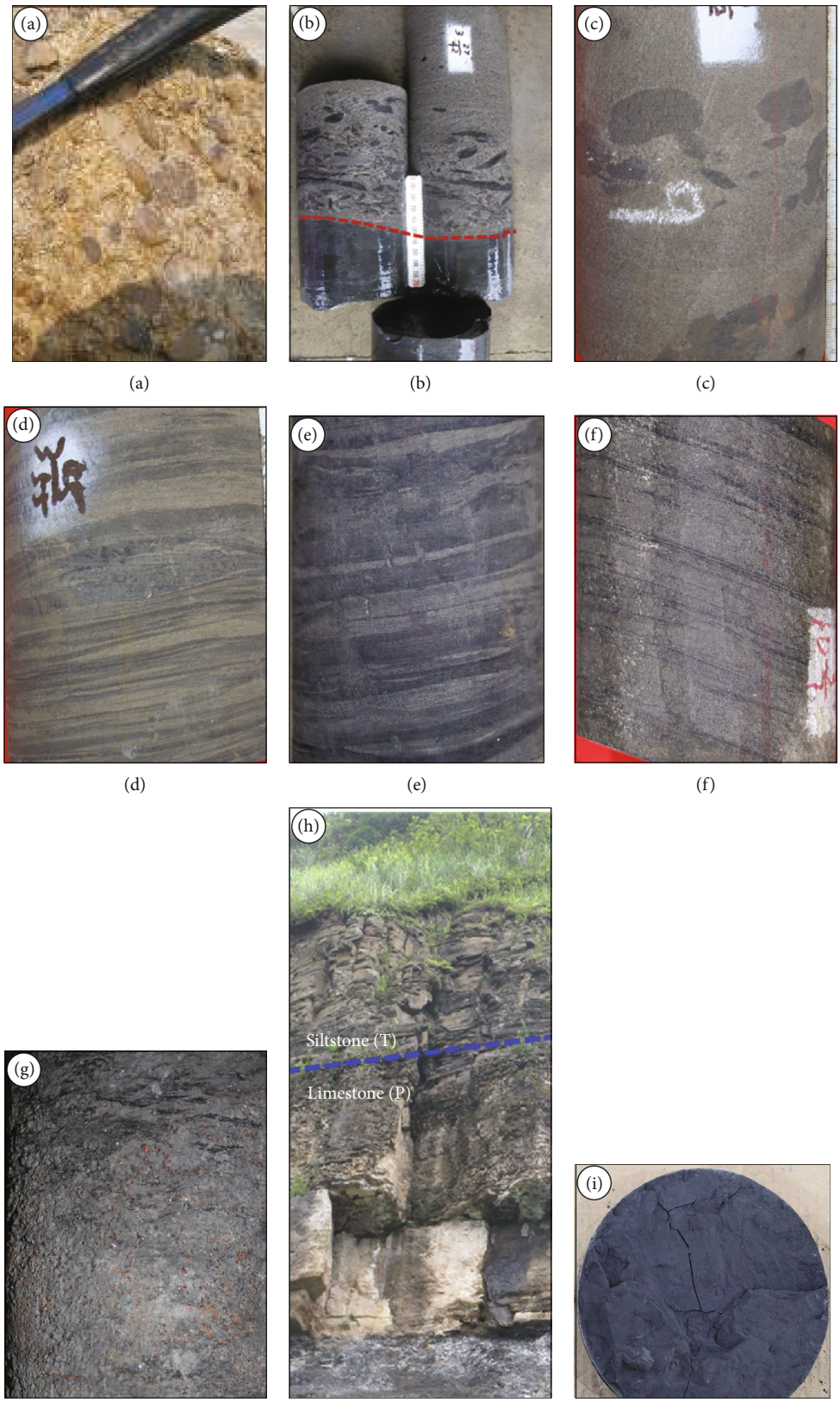

Figure 2: Continued.

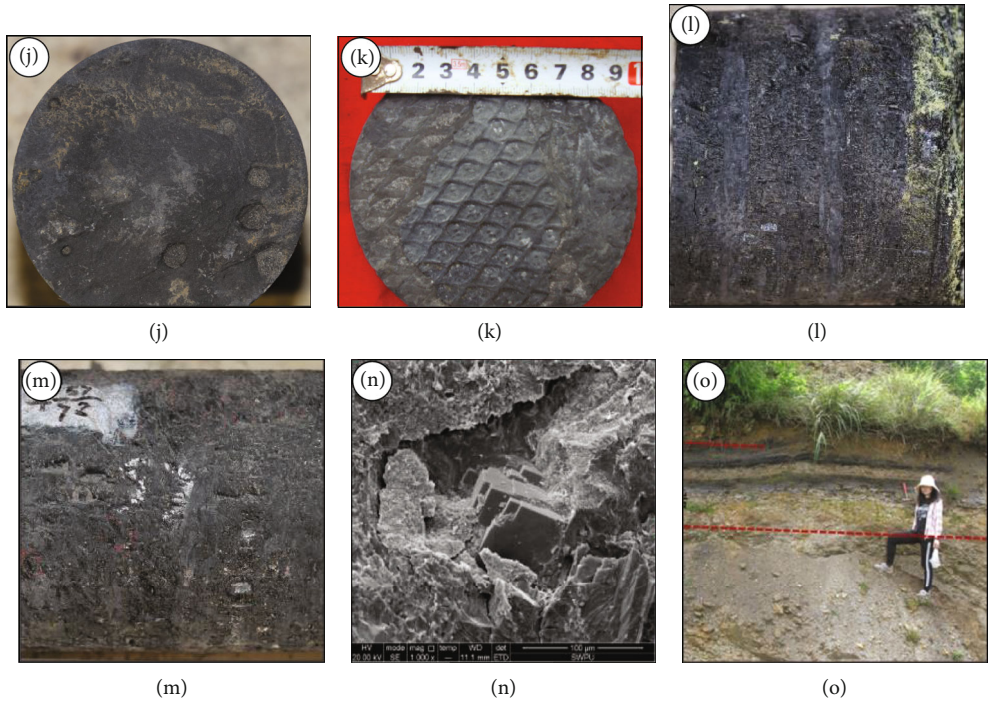

Figure 2: Photographs of the lithology of the Lopingian coal-bearing system in the southern Sichuan area: (a) gray conglomerate, meandering river channel retention sediment, Xunsi section, Junlian; (b) conglomerate-bearing fine sandstone, flattened mud gravel with biaxially aligned tectonics, matrix-supported, average rounded, and poorly sorted, borehole YSL1, 610.5 m in depth, lower member of the Longtan Formation; (c) conglomerate-bearing fine sandstone, flattened mud gravel with biaxially aligned tectonics, matrix-supported, poorly rounded, and poorly sorted, storm event disturbance structure, borehole YSL1, 582.5 m in depth, upper member of Longtan Formation; (d) lenticular bedding sandstone, borehole Z105, 581.56 m in depth, Junlian; (e) lenticular bedding sandstone with well-developed bioturbation structure, borehole YSL152, 581.5 m in depth; (f) tidal bedding-trough-shaped cross-bedded sandstone with well-developed bioturbation structure, borehole YSL152, 582.5 m in depth, Junlian; (g) rhodolitic mudstone with oolitic tectonics, borehole YSL152, 607.5 m in depth, upper member of Longtan Formation; (h) muddy limestone, Xuyong; (i) dark mudstone with marine faunal fossils, borehole YSL1, 610.5 m in depth, upper member of Longtan Formation; (j) dark mudstone with biogenic subduction development, borehole YSL152, 581.7 m in depth, upper member of the Longtan Formation; (k) dark mudstone with Lepidodendron fossils, borehole Z105, 609.3 m in depth, upper member of the Longtan Formation; (l) primary-fractured structural coal with pyrite layer-filled fissures, borehole YSL37, Muai, Junlian; (m) primary-fractured structural coal, borehole YSL37, Muai, Junlian; (n) calcite cement in coal, borehole YSL1, 608.7 m in depth, Muai, Junlian; (o) Bauxitic mudstone, developing pyrite crystals, bottom of Longtan Formation. 10 cm diameter core in borehole YSL1, 5 cm diameter in other cores, geological hammer length about 30 cm.

as the development of surrounding rock lithology; (2) analyze the relationships between coal seam thickness, coal maceral content, ash and sulfur content, surrounding rock lithology, and changes in gas content; (3) compare the variation of gas content at similar burial depths in different sedimentary units; and (4) finally, conclude the dominant factors affecting the variation of gas content from the aspect of sedimentology.

4. Results

4.1. Lithofacies and Depositional Environments

4.1.1. Petrographic Characteristics. The lithological and petrographic characteristics of the coal-bearing strata in the Lopingian of southern Sichuan were described through field outcrop profile measurements and core observations. Six rock types of conglomerate, sandstone, siltstone, mudstone, limestone, and coal are identified and summarized (Figure 2), and twenty lithofacies types were further classified combining sedimentary structure, rock composition and color, and paleontological features (Table 1).

Conglomerates: the conglomerates of the Lopingian in the southern Sichuan area are mainly fine and medium conglomerates, with occasional coarse conglomerates. Medium conglomerates and fine conglomerates are mainly distributed in the lower member of the Longtan Formation, with scour-fill tectonics developed at the bottom and inside and two-way interstratification visible. The thinning sequence upward corresponds to fluvial retention deposition, divergent fluvial retention deposition, or fluvial flood deposition, and the upwardly thickening sequence corresponds to estuarine dam deposition, while the two-way interstratification corresponds to tide-controlled divergent fluvial or tidal channel deposition.

Sandstone: the sandstone in south Sichuan is generally light gray to dark gray in color, and the debris composition is mainly basaltic rock debris. The sandstone filler is mainly

Table 1: Dominant lithofacies of the Lopingian coal-bearing strata in southern Sichuan.

Lithological types	Lithofacies	Lithology	Environmental interpretation
Conglomerate	(1) Conglomerate	Fine- to medium-grained conglomerate, low maturity, thin-bedded	Channel lag deposit
Sandstone	(2) Massive bedded sandstone	Grayish white and gray, thick-bedded, well-sorted, angular-subangular, with basal erosional surface and plant fossils	Fluvial channel deposit, delta plain distributary channel, and mouth bar
	(3) Tabular cross-bedded sandstone	Grayish white and gray, thick-bedded, well-sorted and well-rounded, basal erosional surface	Mouth bar, point bar deposit, and distributary channel
	(4) Wedge cross-bedded sandstone	Gray and brownish gray, thick-bedded, with mudstone gravels and plant fossils, basal erosional surface	Delta plain distributary channel and mouth bar
	(5) Trough cross-bedded sandstone	Gray white, thick-bedded, few gravels, with basal erosional surface, common mud at the bottom	Point bar of fluvial channel, distributary channel, and mouth bar
	(6) Parallel-bedded sandstone	Fine to medium-grained sandstone, gray white, medium and thick-bedded, with parting lineation	Distributary channel and tidal flat deposit
	(7) Wavy cross-bedded sandstone	Grayish white and gray, thick-bedded, with animal and plant fossils, abundant trace fossils	Distributary channel, tidal flat, and flood plain
	(8) Two-way cross bedded sandstone	Grayish white and gray, thick-bedded, with animal and plant fossils, abundant trace fossils	Distributary channel, tidal channel
Siltstone	(9) Horizontally bedded siltstone	Grayish brown-grayish black, thin-bedded, animal and plant fossils with argillaceous inclusion locally	Flood basin, interdistributary bays, delta front, and lagoon
	(10) Wavy cross-bedded siltstone	Light gray siltstone and dark gray mudstone interbedded, visible storm disturbance, and biological disturbance structure	Overbank and tidal flat
Mudstone	(11) Carbonaceous mudstone	Grayish black and black, often pyrite	Peat swamp
	(12) Massive mudstone	Purple and gray black, medium and thick-bedded, with animal and plant fossils, often pyrite and siderite, and occasionally biological fossils	Lagoon, interdistributary bays
	(13) Horizontally bedded mudstone	Gray and gray black, medium and thick-bedded, with animal and plant fossils	Delta plain interdistributary bays, lagoon
	(14) Bauxitic mudstone	Grayish white, thick-bedded	Lagoon
	(15) Root claystone	Gray and white, rich in root fossils	Peat swamp and lagoon
	(16) Sideritic mudstone	Gray and gray black, thick bedding, with high proportion	Lagoon
	(17) Volcanic ash altered claystone	White-light gray, sticky when exposed to water, often as coal seam gangue	Peat swamp and backswamp
Limestone	(18) Bioclastic limestone	Gray, thick-bedded, abundant fossil bioclasts	Carbonate platform
	(19) Muddy limestone	Light gray-dark gray, thick-bedded	Carbonate platform
Coal	(20) Coal	Black, thin-medium and thick-bedded, coal composition is dominated by vitrinite, cleat development	Peat swamp

clay mineral miscellaneous base, including chlorite, kaolinite, montmorillonite, and illite, followed by a small amount of calcareous, siliceous, and rhodochrosite cement. The debris particles are generally rounded, mostly subrounded, and subangular, with average to good sorting.

Siltstone: the siltstone is widely distributed in south Sichuan, with similar clastic composition to sandstone and deeper clastic alteration which is mostly in the form of chloritic clasts. The filler is relatively more than that in sandstone, dominated by cryptocrystalline chlorite and kaolinite fragments, and transitional to mudstone. According to the sedimentary structure, it can be divided into horizontal laminated siltstone interbedded with mudstone, tidally laminated siltstone interbedded with mudstone, soft sedimentary deformed siltstone interbedded with sandstone and mudstone, and rhodolitic siltstone interbedded with mudstone.

Mudstones: Lopingian coal-bearing mudstones are developed in various environments and can be classified as carbonaceous mudstones, dark mudstones, light-colored mudstones, rhodochrosite mudstones, bauxite and bauxite

Table 2: Main depositional systems of the Lopingian coal-bearing rock system in southern Sichuan.

Facies associations	Subfacies	Environments	Lithofacies
Fluvial plain (meandering)	Fluvial channel	Channel lags Point bar	1, 2, 3, 5
	Overbank	Levee Crevasse splay	9, 10
	Flood basin	Backswamp Peat swamp	9, 11, 17, 20
Shallow-water delta	Upper delta plain	Distributary channel Distributary channel levee Crevasse splay Interdistributary bay Peat swamp	2, 3, 4, 5, 6, 9, 12, 13
	Lower delta plain	Distributary channel Distributary channel levee Crevasse splay Interdistributary bay Peat swamp	2, 4, 6, 7, 8, 9, 12, 13
	Delta front	Mouth bar Distal bar	2, 3, 4, 5, 12
Tidal flat-lagoon	Tidal flat	Sandy flat Mixed flat Muddy flat Tidal channel Peat swamp	6, 7, 8, 10, 11, 15, 17, 20
	Lagoon	Lagoon Peat swamp	11, 13, 14, 16, 17, 20

mudstones, root mudstones, and volcanic ash altered claystones according to the differences in composition, color, and genesis of the mudstones. The clay mineral composition is mainly chlorite, kaolinite, illite, montmorillonite and illite-montmorillonite mixed-layer minerals, containing quartz, rhodochrosite, pyrite, and other minerals, with horizontal lamination and plant or marine animal fossils. When the rhodolite mudstone and siltstone are interstratified, it can form a very characteristic "row of bones layer."

Coal: the main coals of the Lopingian in southern Sichuan are mainly formed in the peat swamp environments in the delta plain divergent interdistributary bays and lagoon-tide flat environment. It is mainly anthracite, and the macroscopic coal rock type is mainly semibright to semidark coal, with strong luster, adamantine luster, and metallic luster. These coals are mostly developed striated structure or linear structure and few with flake structure. Pyrite, calcite, and quartz are mostly filled in coal fissures or distributed along the coal seam strips.

Limestone: the Lopingian limestone was mainly developed in the Changxing Formation and dominated by tuffs. It is generally dark gray-light gray in color, mainly medium-thick bedded, locally thin bedded, or lenticular, and occasionally has siliceous nodules, oolitic structures, sutures, and other sedimentary structures. The muddy tuffs are mainly composed of illite and eumonite, with occasional chlorite, ranging from 10% to 50%, mostly in thin laminations or bands, interspersed with bioclastic tuffs or dark mudstones, containing marine animals. Bioplastics are abundant and mainly are algae, followed by foraminifera, Fusulinida, mesomorphs, brachiopods, bivalves, sea lily stems, chrysocolla, etc.

4.1.2. Sedimentary Environment. Based on the combination of lithofacies and their spatial distribution, the environment of the Lopingian in the study area was identified as a sea-land transitional craton basin environment consisting of river flood plains, shallow-water deltas, and tidal flat-lagoon sedimentary systems (Table 2).

(1) Facies Association A: Fluvial Plain. The fluvial plain was mainly developed in the western part of Junlian and Yanjin areas in the middle and upper member of Xuanwei Formation. It can be divided into fluvial channel, overbank, and flood plain deposit. According to the characteristics of channel sand, it can be divided into braided river and meandering river system, corresponding to the evolution of from early river life to late.

(2) Facies Association B: Shallow-Water Delta. The river-controlled upper delta plain is represented by the lower member of the Longtan Formation. Its typical characteristics are the high degree of superposition of sand bodies upward in the distributary channel and the intertwined network form on the plane. Marine animal fossils and thin siderite layers are visible in the distributary bay, with general low

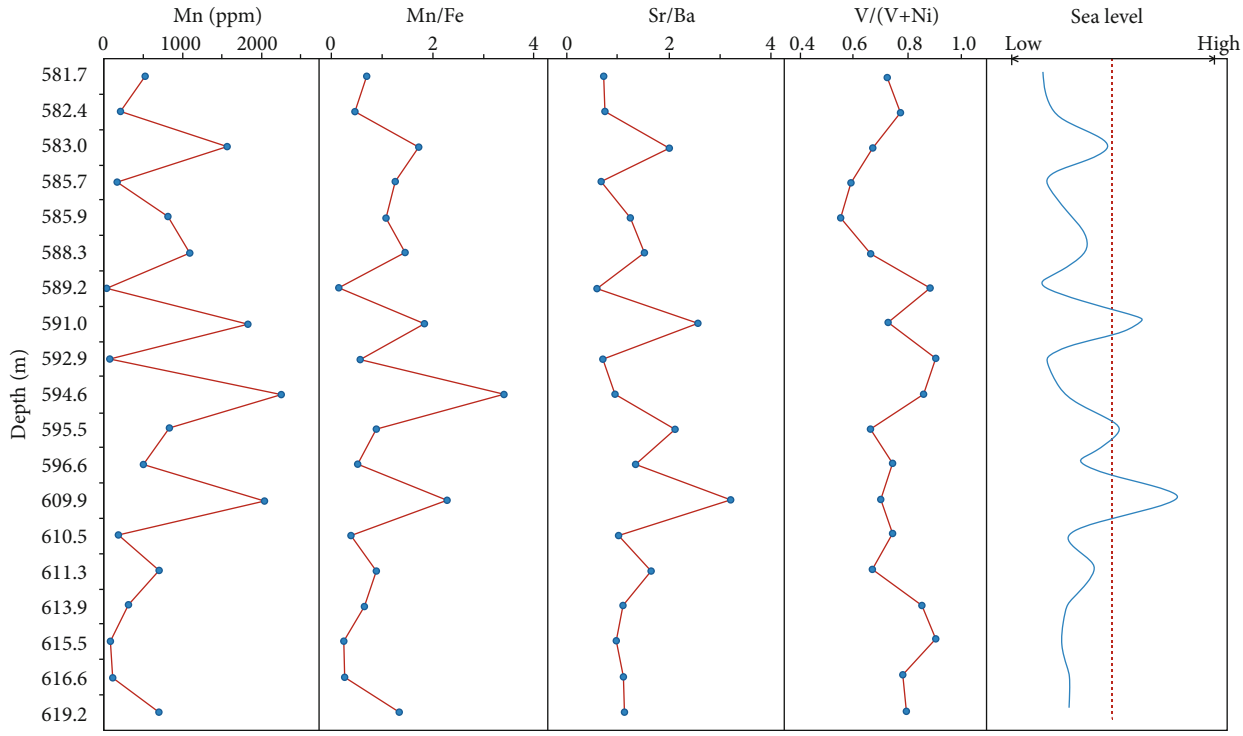

Figure 3: Trace element geochemical analysis test of the Lopingian paleooxygen phase of the borehole YSL1.

ash and sulfur content in the coal bed. The lower delta plain has a relatively low degree of superposition of sand bodies in tidal-controlled distributary channels, with rich sea greenstone and more developed tidal bedding and bidirectional cross-bedding. Abundant marine animal fossils are visible in the distributary bays; There is a transition zone between the upper and lower delta plains, and the delta plains of the transition zone are affected by the rivers and tides, forming relatively stable peat swamp environment and the horizontally stable coal seams with large thickness.

The delta front includes mouth bars and distal bars. The shape of the mouth bar sand is mostly lenticular in the section and elliptical in the plane parallel to the direction of the tidal current, which is the result of the progradation of the mouth bar. The distal bar has a finer grain size than the mouth bar and is farther away from the delta plain.

(3) Facies Association C: Lagoon–Tidal Flat. The barrier unit corresponding to lagoon with brackish water in the transitional environment of Lopingian coal-bearing series is the transitional barrier sand dam (beach). In addition, the reefs in the basin edge and the tidal sand in epeiric sea shelf can also act as barriers. Due to the extremely gentle slope of the epeiric sea shelf, the direct distance between the lagoon and barrier unit may be so long; thus, the vertical sedimentary sequence of them might not be in direct contact, and the barrier sand bar can be sandwiched between carbonate platform deposits or between carbonate platform deposits and tidal flats deposits, and lagoon sediments can also be sandwiched in tidal flats.

Tidal flat deposits are mainly distributed on the outer edge of shallow-water delta facies belts. Sandstone, siltstone, mudstone, and other deposits from shallow-water deltas are transformed by tidal action to form subtidal tidal channels and intertidal tidal flats. Tidal flats mostly change into fining sedimentary sequence upward comprising sand flat-mixed flat-mud flat. The supratidal zone is generally a salt marsh environment, and peat swamps can develop.

4.1.3. Geochemical Analysis. The Sr/Ba ratio value is a geochemical indicator to distinguish terrestrial and marine sedimentary environments [28]. The geochemical index V/(V + Ni) shows that Lopingian coal-bearing series was formed in an oscillatory anoxic depositional environment, and the paleosalinity index Sr/Ba shows that the Lopingian was a semisaline-brackish water environment, where Mn elements could exist in seawater in a relatively stable manner as Mn^{2+}, and Fe was easily oxidized to Fe^{3+}. Most of the Fe element transported to the ocean that appeared in suspension. Mn element content and Mn/Fe ratio indicate that the sea level changed frequently during the Lopingian period (Figure 3).

4.2. Sequence Stratigraphic Framework. In this paper, the sedimentary sequence classification scheme proposed by Van Wagoner (1987) was adopted for the establishment of the sea-land transitional deposits of the inner craton basin in Junlian mining area [29, 30]. The boundaries of sedimentary sequence are the terrestrial unconformity at the basin margin and the corresponding integration at the basin center [31]. Based on the sedimentary characteristics of the

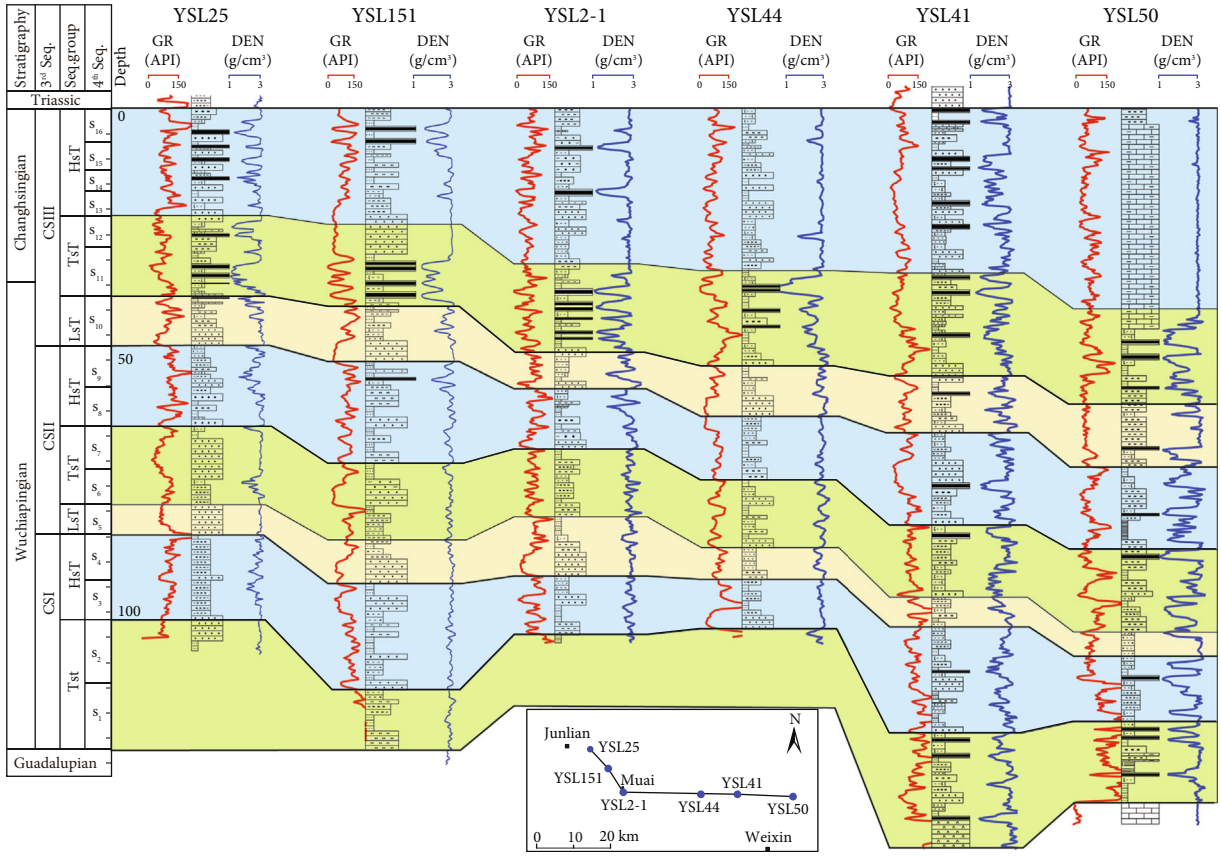

Figure 4: Stratigraphic framework of the Lopingian stratigraphy in the Junlian of southern Sichuan.

Lopingian coal-bearing series in Junlian area, the key stratigraphic interfaces reflecting sea-level changes include regional exposed unconformity, river cut valley erosion basement, paleosols, sedimentary facies transitional surfaces, and coal seams, and four third-order stratigraphic interfaces can be identified.

According to the superimposition style of the fourth-order sequence (progradation, aggradation, and retrogradation) or the shoreline migration characteristics corresponding to the fourth-order largest ocean flooding surface, the third-order composite stratigraphic sequence can be further divided into Lowstand Systems Tracts (LST), Transgressive Systems Tract (TST), and Highstand Systems Tract (HST). These three third-order composite stratigraphic sequences CSI, CSII, and CSIII are divided ascendingly based on the four third-order stratigraphic interfaces, among which CSIII includes seven fourth-order stratigraphic sequences, CSII includes five fourth-order stratigraphic sequences, while due to the restricted development and diachronism of the bottom surface of the Lopingian in some terrestrial sedimentary areas, CSI include up to four fourth-order sequences in marine sedimentary areas (Figure 4).

4.3. Lithofacies Paleogeography. In this paper, the petrographic paleogeographic analysis is conducted only for CSIII, which is based on the sandstone/mudstone contour map with reference to the single-factor parameter contours of stratigraphic thickness, sandstone thickness, mudstone thickness, limestone thickness, etc. The sedimentary zones of CSIII are spreading nearly east-west, with the river alluvial plain distributed to the west in Gaoxian-Junlian area and the shallow-water delta in Junlian-Gongxian area, respectively. The river-controlled deltaic plain was distributed in the area of Junlian-Gongxian, and the tide-controlled deltaic plain was spread in the eastern part of the deltaic plain, and the deltaic foreland-tide flat zone was located in the area of Weixin, and the tide flat-restricted platform deposit was developed in eastern part of Xingwen-Xuyong (Figure 5).

4.4. The Characteristics of Coal Seam Distribution, Coal Macerals, and Coal Quality

4.4.1. Coal Seam Distribution. Coal seams are developed when the growth rate of basin accommodative space is slightly greater than the peat accumulation rate. The Lopingian sedimentary environments in Junlian area mainly comprise river alluvial plains, shallow-water deltas, and lagoon-tidal flat environments. Junlian area mainly develops C_7 and C_8 and C_2 and C_3 coal seams, of which the thickness of $C_7 + C_8$ and $C_2 + C_3$ coal is 3-10.5 m (Figure 6) and 1-4.5 m (Figure 7), respectively. These thick coal seams were mainly developed in the peat swamp environment of inter-distributary bays in the upper and lower delta plain and tidal flats in Muai and Zhenzhou. Coal seams are generally developed in the fluvial plain environment in the western part of the Junlian coalfield.

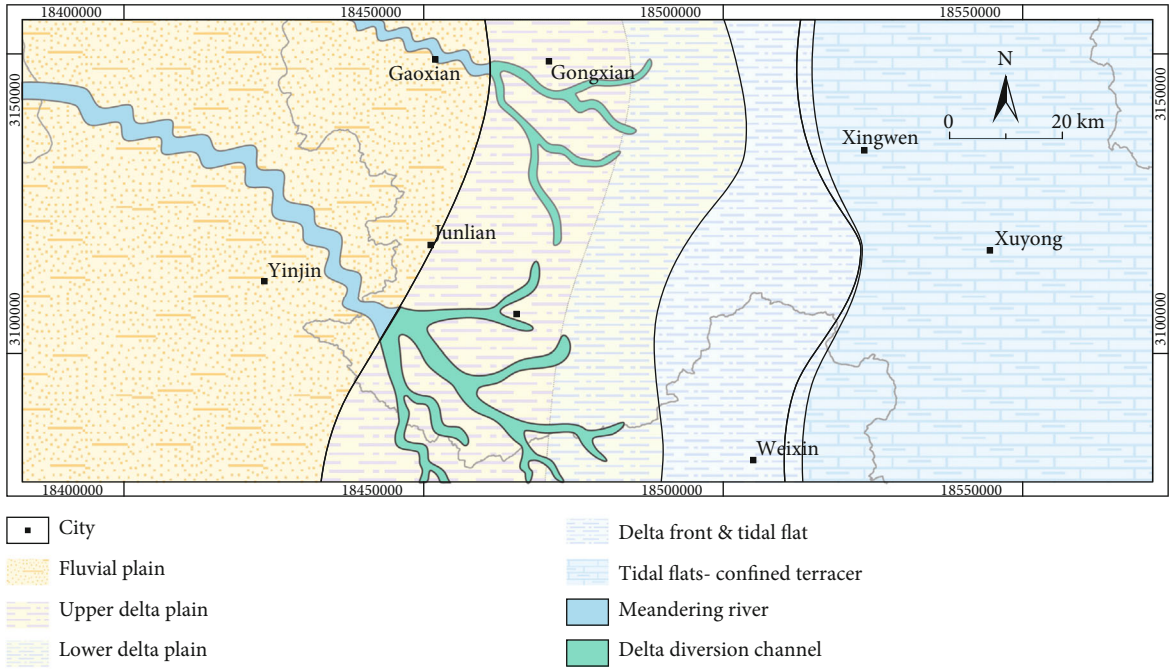

Figure 5: The Lopingian CSIII petrographic paleogeography map of Junlian.

4.4.2. Coal Maceral and Coal Quality. The organic maceral components not only affect the pore structure and pore volume of coal reservoirs but also affect the adsorption capacity and desorption rate of coal for methane [32, 33]. Ten exploration reports and drilling core test results show that the organic maceral components in the Junlian area are mainly vitrinite group, followed by inertinite group, and liptinite group content is tiny. The average content of the vitrinite group in C_7 coal seam is 71.11%, and the average content of the inertinite group is 21.51%. The total amount of organic matter accounts for 92.62% of the microscopic coal composition. The vitrinite content of the C_8 coal seam averages 70.13%; the average content of the inertinite group is 23.50%. The total amount of organic matter accounts for 93.63% of the microscopic coal composition. Compared with Junlian coals, vitrinite contents in coals of Xuyong area are low, but other characteristics of coals are basically similar (Table 3).

The R_O is an effective indicator of the coal coalification degree. According to the analysis results of coal exploration reports, the metamorphism level of the Lopingian coal seams in the Junlian area is generally as high as the lean coal—anthracite. The R_O values of C_7 and C_8 coal seams are between 2.86% and 3.84%, corresponding to anthracite (Figure 8). On the whole, R_O values of the main mineral coal seams in this region show a decreasing trend from west to east. Among these values, the borehole YSL6 has a minimum value of 2.86% and the borehole YSL11 has a maximum value of 3.84%.

The R_O values of main coal seams C_2 and C_3 in the study area are between 2.77% and 3.74%, equal to anthracite (Figure 9). It shows a decreasing trend of main coal seams C_2 and $C_3$$R_O$ values from west to east in this region on the whole, among which the borehole YSL6 has a minimum value of 2.77% and the borehole YSL11 well has a maximum value of 3.74%.

4.5. Spatial Distribution of Gas Content. Based on the data from 39 CBM wells and borehole data, the gas-bearing characteristics of the main coal seams C_7 and C_8 and C_2 and C_3 were statistically analyzed, respectively. The R_O values of both C_7 and C_8 coal seams in the southern Sichuan area are greater than 2.86% representing a high coal rank, and the gas content is greater than 8 m^3/t in most areas, with low level only in the stripping areas and the areas south of borehole YSL4 (Figure 10). Among them, the gas content of C_7 coal seam in the Junlian area ranges from 6.96 to 18.94 m^3/t, with an average of 14.19 m^3/t, and the gas content of coal seam C_7 in the core area of Muai is more than 16 m^3/t. The gas content of the C_8 coal seam is similar to that of the C_7 coal seam, and the gas content of the C_8 coal seam is between 4.9 and 20.45 m^3/t, with an average of 13.22 m^3/t. The gas content of the C_8 coal seam in the Muai area also exceeds 16 m^3/t. In summary, the C_7 and C_8 coal seams can be considered as the same gas-bearing system.

The R_O values of both C_2 and C_3 coal seams in the study area are greater than 2.77%, indicating a high rank, and the gas content in most areas is also greater than 8 m^3/t, and those in the stripping area and the area northwest of the borehole YSL25 are less than this level (Figure 11).

5. Discussion

5.1. Influence of Sequence Stratigraphy and Paleogeography on CBM Accumulation. The coal aggregation is influenced by the comprehensive influence of the stratigraphic

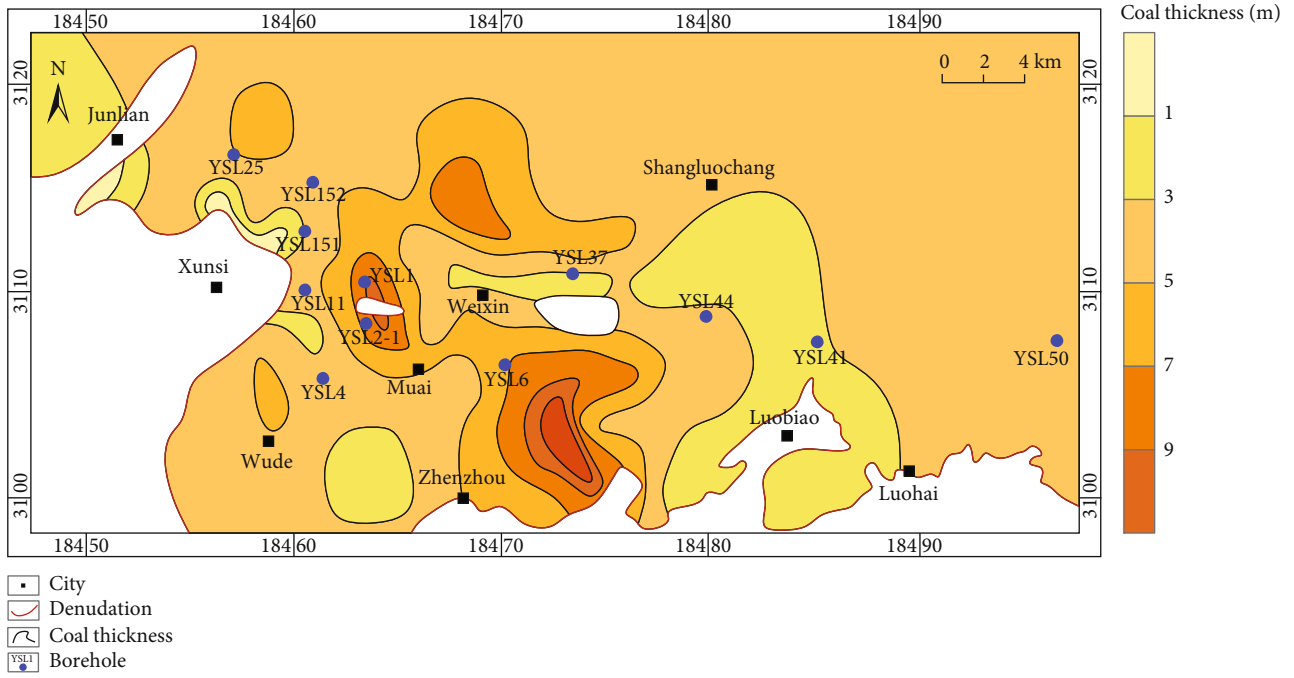

Figure 6: $C_7 + C_8$ coal seam thickness contour of Junlian.

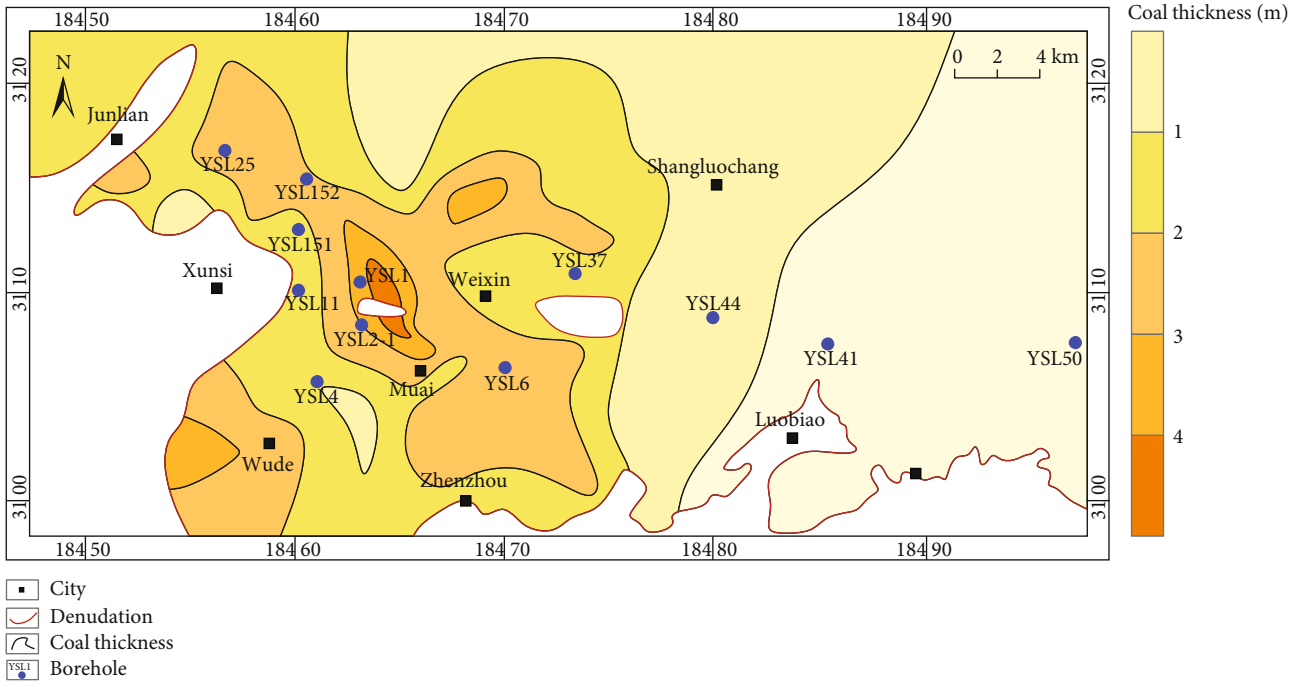

Figure 7: $C_2 + C_3$ seam thickness contour of Junlian.

framework and the paleogeographic depositional environment. In different paleogeographic backgrounds of different stratigraphic frameworks, R_P (rate of peat accumulation) and R_A (increasing rate of accommodation) have different performances, and the spatial distribution of coal seam thickness in the vertical and planar directions has different characteristics [18]. The R_A-R_P balance in the stratigraphic frameworks is most significantly influenced by sea-level change, differential basin subsidence, and sedimentary supply in the east-west direction. The thickness of coal seams generally has a positive influence on the gas content of coal seams [34], and there is an overall positive correlation between the gas content and coal thickness in the study area. Coal seam thickness not only controls the gas potential of

Table 3: Coal maceral composition and coal quality characteristics in southern Sichuan.

Study area	Coal	Vitrinite group (%)	Inertinite group (%)	TOC (%)	Mineral (%)	$R_{O,max}$ (%)	Coal types
Junlian	C_7	71.11	21.51	92.62	7.38	2.90	Anthracite
	C_8	70.13	23.50	93.63	6.37	2.83	Anthracite
Xuyong	C_7	37.05	41.85	78.90	21.10	2.37	Anthracite
	C_8	39.06	50.48	89.54	10.46	2.58	Anthracite

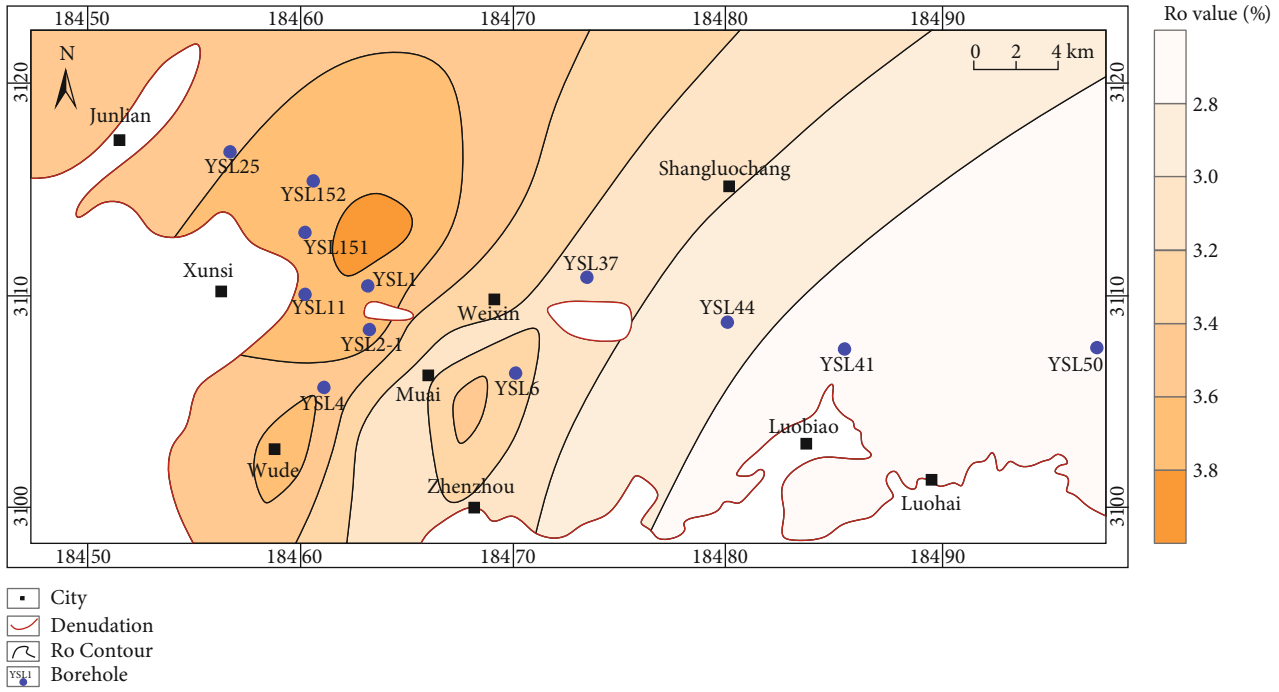

Figure 8: R_O contour map of Lopingian $C_7 + C_8$ coal seam in Junlian mining area.

coal reservoirs but also has an impact on CBM preservation. In the case of unsatisfactory storage conditions for the roof and floor of the coal seam, the thickness of the coal seam has a more significant influence on the gas content.

Under the condition of offshore coal accumulation on the margin of the craton epeiric sea, most of river alluvial plains and river-controlled upper delta plains near the source area were in a compensation or overcompensation state, due to the relatively sufficient land source supply, that is, $R_P > R_A$. When the base level rise rate and the basin structure subsidence rate were fast, the accommodation space increased rapidly, and R_P and R_A could maintain a stable equilibrium state for a long time. Therefore, thick coal seams generally developed near the MFS (maximum flooding surface) or in the HST of CSIII and CSII. The coal accumulation center in the delta system with relatively low accommodation space was generally located in the lower delta plain or the interdistributary bays of the upper and lower delta plain transition zone.

According to the analysis results of the sequence stratigraphic framework in the east-west direction, it shows that, from CSI and CSII upward to CSIII, coal accumulation gradually increased and also the thickness of coal seams. During the CSI stage, coal seams were mainly developed in TST and HST, mainly distributed in the Xuyong area on the north and south sides of the north Guizhou-south Sichuan uplift belt, where the subsidence rate was relatively high. The thickness of the coal seams ranged from 0.2 to 5.69 m and gradually pinched westward. The coal-accumulating environment was mainly lagoon-tidal flat environment, with low ash content and high sulfur content.

In the CSII stage, the coal accumulation effect was stronger than that in the CSI stage and developed in both TST and HST. The thickness of the coal seam ranges from 0.1 to 7.67 m and gradually decreases from east to west also with decreased number of coal seams. The coal-accumulating environment was tidal-controlled lower delta plain and the interdistributary bay of the upper and lower delta plain transition zone, with high ash content and medium sulfur content.

During the CSIII stage, coal accumulation was the strongest, and coal accumulation was generally developed in the whole area. The thickness of the coal seam ranges from 1 to 13 m and increases first and then decreases from east to

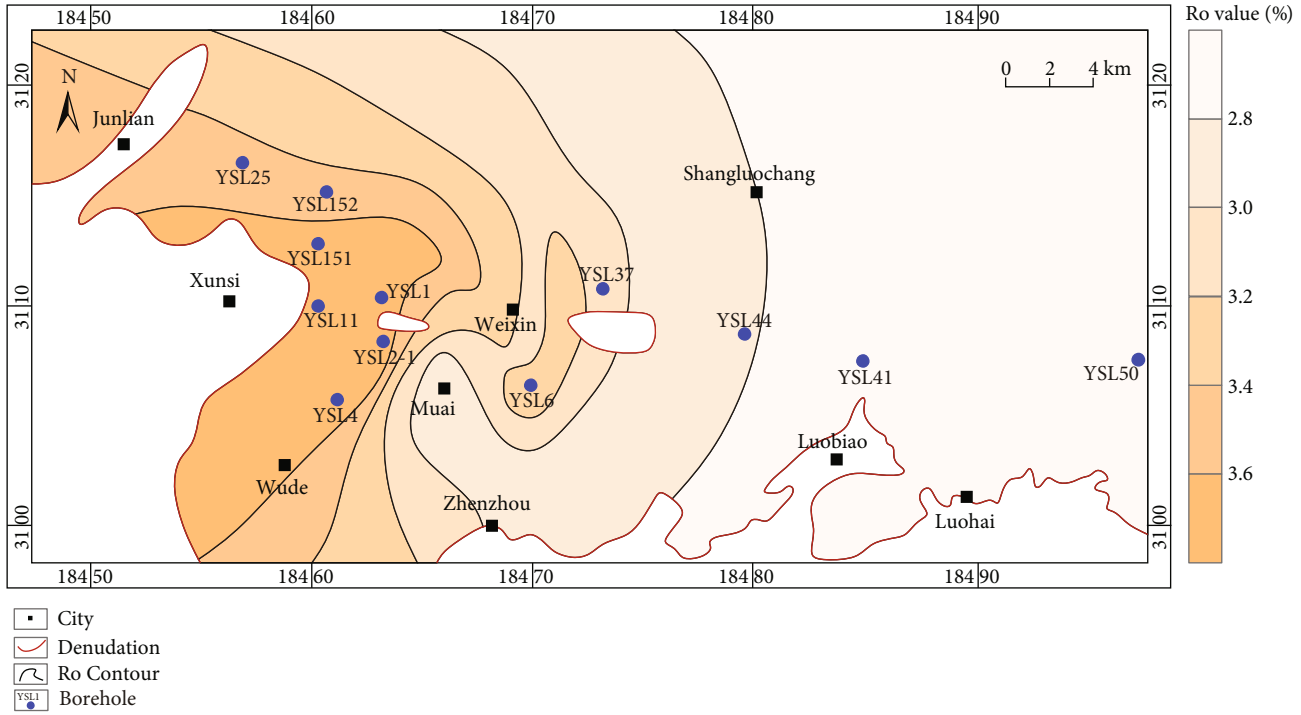

FIGURE 9: R_O contour map of Lopingian $C_2 + C_3$ coal seam in Junlian mining area.

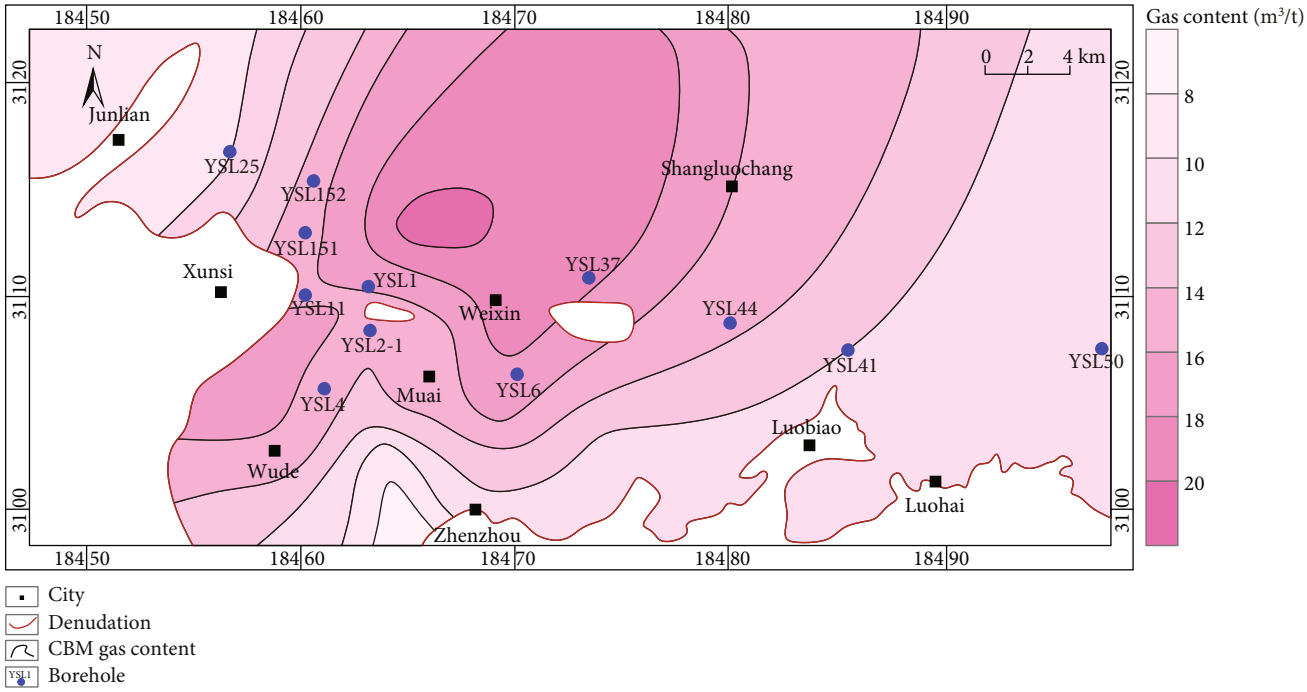

FIGURE 10: Gas-bearing contours of the Lopingian $C_7 + C_8$ coal seam in the Junlian mine area.

west in the sequence stratigraphic framework. The development layer of coal seams gradually increases from LST to TST finally to HST east to west, synchronized with the large-scale transgression process in the Changxing period. A thin coal seam of 1 m developed in LST in Xuyong area; two coal layers were developed in TST, with a total thickness of 3 m; and coal seams in HST were not developed. These coals were formed in the lower delta plain-tidal flat environment, with high sulfur content and medium ash content. The TST in Junlian area mainly develops C_7 and C_8 coal

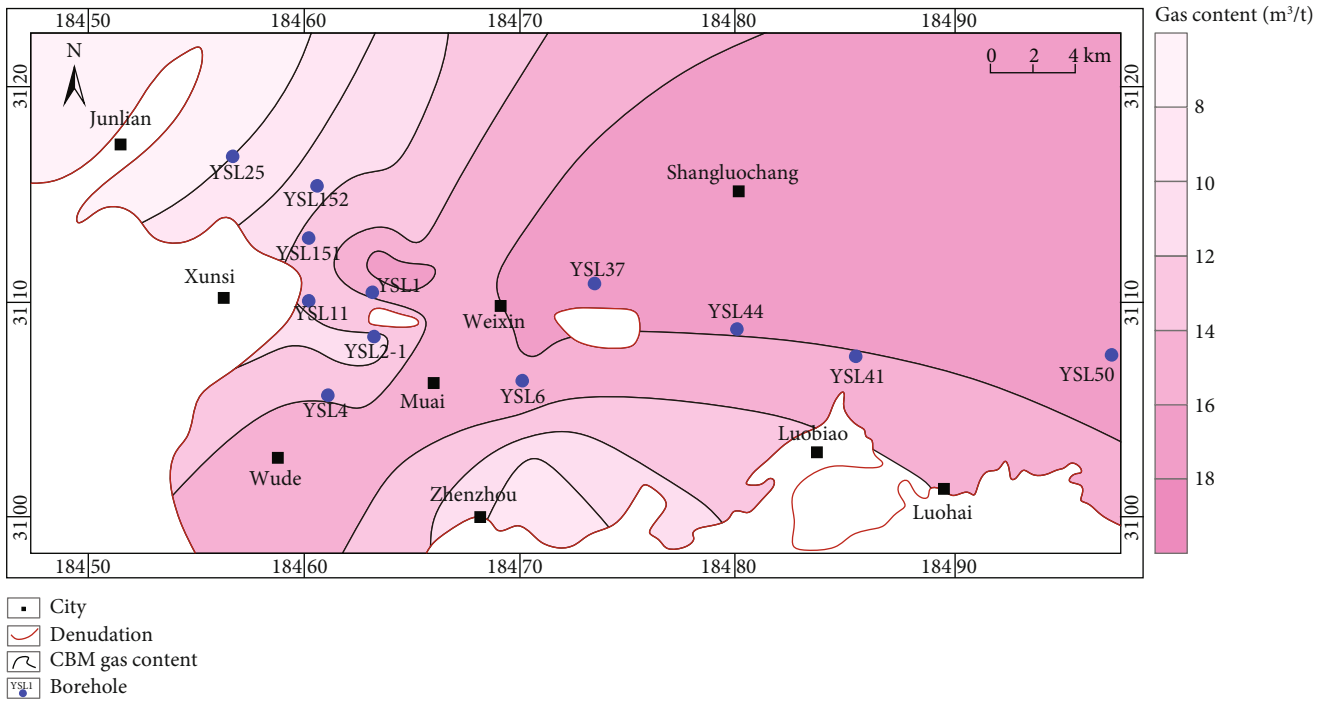

Figure 11: Gas-bearing contours of the Lopingian Unit $C_2 + C_3$ coal seam in the Junlian mine area.

seams, with characteristics of large coal seam thickness and good lateral continuity. The maximum thickness of the coal seam can reach 6 m, with an average of about 2.5 m. In stage of HST, it mainly develops C_2, C_3, and C_7 coal seams, among which the C_7 coal seam has the largest thickness and also the best horizontal continuity as well as the maximum coal thickness reaching 13 m with the average about 5.6 m. These coals were formed in the transition zone of the upper and lower delta plains, with medium ash content and medium sulfur content. The coal seams in the western part of Junlian area were mainly developed in the floodplains of the river alluvial plains of HST and the peat swamps in the interdistributary bays of the upper delta plains, with high ash content and low sulfur content.

5.2. Influence of Fold Structure on CBM Accumulation. Fold structures have a significant control effect on the migration and accumulation of CBM [35, 36]. On the one hand, coalbed in the fold structure rises and the static pressure decreases accordingly, which is conducive to the desorption of CBM. On the other hand, fissures developed in the anticline and syncline axis with stronger ground stresses, coal reservoir porosity and permeability will increase, and reservoir pressure decreases, which is also conducive to the desorption of CBM. The barrier-type fold structures with open syncline and closed anticline were mostly developed in southern Sichuan. The two flanks and the axis above the neutral plane of the syncline structure are compressive stress fields, and below the neutral surface are tensile stress fields, and because of the deep buried depth of coal seams, only a few open fissures are produced and part of the stress is released to form a relatively low-pressure area. Therefore, the two flanks and the axis above neutral surface of the syncline are conducive to the storage and accumulation of CBM. In particular, the axis of the syncline is often an area with high gas content. The secondary anticlines without weathering and denudation are also conducive to the enrichment and accumulation of CBM. The secondary anticlines in the Junlian area are located on the two flanks of a large, wide, and gentle compound syncline. The anticline is small in amplitude, the flanks are gentle, and the fissures are not developed. Gas formed in coal seams migrates upwards, forming free gas reservoirs under favorable sealing conditions. Above the neutral surface of the anticline axis, there is a tensile stress field, which is a low-pressure zone, with developed fissures and increased coal seam permeability. The large accommodation space is conducive to the accumulation of CBM.

5.3. Enrichment Model of CBM in the Junlian Coalfield. Sedimentary facies belts have a significant control effect on the development of the gas-bearing system combination. From the river alluvial plain to the tidal flat-restricted platform environment, the CBM gas-bearing system combination is becoming more and more complicated [37]. The Late Permian coal-bearing strata in the study area are dominated by delta and tidal flat deposits. The distribution of the depositional system has obvious east-west zoning characteristics, which are river alluvial plain, delta, tidal flat-lagoon, and tidal flat-carbonate platform from west to east.

The coal-bearing strata receive atmospheric precipitation in the outcropping zone of the syncline flank to form groundwater, which flows from the flank to the axis. The hydraulic effect is gradually weakened, and eventually, a

groundwater retention zone is formed in the syncline core. Groundwater runoff produced a hydraulic plugging effect on the escape of CBM, and the syncline core area is conducive to the accumulation of CBM [38]. The Muai core exploration and development area in Junlian is mainly composed of a wide and gentle syncline. The groundwater flow channels provided by the two flanks of the syncline are strong runoff areas, and the coalbed water gradually converges downwards to the retention area at the syncline axis. During the flow of groundwater, the direction of runoff is opposite to the upward escape of CBM, forming a hydrodynamic blockage. The groundwater in the retention zone gradually increases, and the pressure of the coal reservoir increases correspondingly to form a confined groundwater zone. Affected by the lithology of the clastic rock and the small stratum dip angle, the groundwater flow in the coal-bearing strata is very limited and weak, forming a medium-weak runoff zone. CBM is blocked by water and caprocks, and it is easy to form a confined water-blocked CBM reservoir.

Large-scale anticline structures are not conducive to the accumulation of CBM, and the axis of secondary anticlines can work as free gas accumulation areas. Some secondary anticlines developed in the Junlian mining area; within them, the coal seams are buried at a depth of about 300 m with mostly mudstone roof, which exhibits high plasticity. The tensile stress will only increase the plastic deformation and not produce open cracks; thus, the roof of coal still maintains good sealing performance. Under the action of compression stress in the anticline flanks, the coal reservoir pressure increases. Affected by the tectonic stress, the CBM in the anticline flanks migrates to the upper part, forming a CBM enrichment area in the secondary anticline axis. At this time, CBM is still enriched above the neutral surface, and free gas accounts for a considerable proportion. The core of the secondary anticline has a high degree of groundwater salinity (>10000 mg/L) with slow groundwater flow, forming a hydraulic seal on the CBM, which is conducive to the accumulation of CBM.

6. Conclusion

(1) Six rock types and twenty lithofacies types were identified of the Lopingian coal-bearing series in southern Sichuan. Four types of sedimentary systems were summarized, and five key sequence interfaces were identified. Combined with the spatial distribution of regional marine markers, fourteen to sixteen fourth-order sequences and three third-order sequences were divided. The stratigraphic framework of the Lopingian coal-bearing series was established

(2) The third-order sequence CSIII paleogeography features from west to east are alluvial plains, deltas, lagoon-tidal flats, and limited carbonate platforms. Thick coal seams are mainly developed in the sedimentary environment of tidal flats, delta plains, and floodplains behind banks. The vitrinite content in the continental coal-accumulating environment is significantly higher than that in the transitional coal-accumulating environment, while the inertinite content is the opposite

(3) The gas content of Lopingian coal seams in the Junlian area, which is generally higher than 8 m^3/t, is closely related to coal seam thickness. Relative sea-level changes and sedimentary paleogeography affect the spatial distribution of coal-accumulating sedimentary environment and the degree of coal seam development, which in turn control gas generation potential and preservation conditions of CBM

(4) CBM accumulation is significantly controlled by the fold structure. The hydraulic plugging effect makes the syncline core favorable for CBM accumulation. In addition, favorable geostress conditions enable the secondary anticline to become a favorable area for CBM accumulation when the sealing conditions are better

Data Availability

This research established a database consisting of 39 boreholes and outcrop profiles for coal accumulation and CBM enrichment rule analysis of the Lopingian coal-bearing series.

Conflicts of Interest

The authors declare that they have no conflicts of interest.

Acknowledgments

This study was supported by the Open Fund (PLC 20210302) of State Key Laboratory of Oil and Gas Reservoir Geology, Chengdu University of Technology, and Science and Technology Plan Project of Education Department of Jiangxi Province (GJJ200723). We also thank PetroChina Zhejiang Oilfield Company for providing the basic data used for research.

References

[1] M. Mastalerz, "Coalbed methane: reserves, production, and future outlook," *Future Energy*, 145–158, 2014.

[2] R. C. Milici, J. R. Hatch, and M. J. Pawlewicz, "Coalbed methane resources of the Appalachian basin, eastern USA," *International Journal of Coal Geology*, vol. 82, no. 3-4, pp. 160–174, 2010.

[3] P. A. Hacquebard, "Potential coalbed methane resources in Atlantic Canada," *International Journal of Coal Geology*, vol. 52, no. 1-4, pp. 3–28, 2002.

[4] P. Cienfuegos and J. Loredo, "Coalbed methane resources assessment in Asturias (Spain)," *International Journal of Coal Geology*, vol. 83, no. 4, pp. 366–376, 2010.

[5] C. Z. Jia, M. Zheng, and Y. F. Zhang, "Unconventional hydrocarbon resources in China and the prospect of exploration and development," *Petroleum Exploration and Development*, vol. 39, no. 2, pp. 139–146, 2012.

[6] D. Lin, J. P. Ye, Y. Qin, and S. H. Tang, "Characteristics of coalbed methane resources of China," *Acta Geologica Sinica (English edition)*, vol. 74, no. 3, pp. 706–710, 2000.

[7] Z. T. Tan, S. L. Wang, and M. Lu, "Current status and prospect of development and utilization of coal mine methane in China," *Energy Procedia*, vol. 5, pp. 1874–1877, 2000.

[8] X. B. Su, X. Y. Lin, M. J. Zhao, and Y. Song, "The upper Paleozoic coalbed methane system in the Qinshui basin, China," *AAPG Bulletin*, vol. 89, no. 1, pp. 81–100, 2005.

[9] C. G. Shan, T. S. Zhang, X. Liang et al., "Influence of chemical properties on CH_4 adsorption capacity of anthracite derived from southern Sichuan Basin, China," *Marine and Petroleum Geology*, vol. 89, pp. 387–401, 2018.

[10] Y. Zhao, T. F. Sun, M. Z. Wang et al., "Research on the production decline law of Junlian coalbed methane development test well," *Chemistry and Technology of Fuels and Oils*, vol. 56, no. 4, pp. 638–645, 2020.

[11] C. G. Shan, T. S. Zhang, X. Liang et al., "On the fundamental difference of adsorption-pores systems between vitrinite- and inertinite-rich anthracite derived from the southern Sichuan basin, China," *Journal of Natural Gas Science and Engineering*, vol. 53, pp. 32–44, 2018.

[12] Y. Kang, J. Fan, P. Liu, J. S. Du, and D. Y. Jiang, "Permeability evolution in tectonic coal: the roles of moisture and pressurized water-injection," *Greenhouse Gases: Science and Technology*, vol. 11, no. 4, pp. 633–646, 2021.

[13] D. Marchioni, M. R. Gibling, and W. Kalkreuth, "Petrography and depositional environment of coal seams in the Carboniferous Morien Group, Sydney Coalfield, Nova Scotia," *Canadian Journal of Earth Sciences*, vol. 33, no. 6, pp. 863–874, 1996.

[14] R. Deschamps, S. O. Sale, B. Chauveau, R. Fierens, and T. Euzenc, "The coal-bearing strata of the Lower Cretaceous Mannville Group (Western Canadian Sedimentary Basin, South Central Alberta). Part 1: stratigraphic architecture and coal distribution controlling factors," *International Journal of Coal Geology*, vol. 179, pp. 113–129, 2017.

[15] R. Nakano, N. Takebe, M. Ono et al., "Geological and hydrogeological controls on the accumulation of coalbed methane in the Weibei field, southeastern Ordos Basin," *International Journal of Coal Geology*, vol. 121, pp. 148–159, 2014.

[16] H. Xu, D. Z. Tang, D. M. Liu et al., "Study on coalbed methane accumulation characteristics and favorable areas in the Binchang area, southwestern Ordos Basin, China," *International Journal of Coal Geology*, vol. 95, pp. 1–11, 2012.

[17] L. Y. Shao, C. Zhang, Z. M. Yan et al., "Sequence- palaeogeography and coal accumulation of the Late Permian in South China," *Journal of Palaeogeography*, vol. 18, no. 6, pp. 905–919, 2016.

[18] L. Y. Shao, X. T. Wang, J. Lu, D. D. Wang, and H. H. Hou, "A reappraisal on development and prospect of coal sedimentology in Chian," *Acta Sedimentologica Sinica*, vol. 35, no. 5, pp. 1016–1031, 2017.

[19] C. A. Shan, T. S. Zhang, J. J. Guo, Z. Zhang, and Y. Yang, "Characterization of the micropore systems in the high-rank coal reservoirs of the southern Sichuan Basin, China," *AAPG Bulletin*, vol. 99, no. 11, pp. 2099–2119, 2015.

[20] H. Wang, L. Y. Shao, L. M. Hao, and P. F. Zhang, "Sedimentology and sequence stratigraphy of the Lopingian (Late Permian) coal measures in southwestern China," *International Journal of Coal Geology*, vol. 85, no. 1, pp. 168–183, 2011.

[21] S. Li, D. Z. Tang, Z. J. Pan, and H. Xu, "Evaluation of coalbed methane potential of different reservoirs in western Guizhou and eastern Yunnan, China," *Fuel*, vol. 139, no. 1, pp. 257–267, 2015.

[22] C. L. Gu, "Geological characteristics and prospect evaluation on coal-seam gas in East Yun nan and West Guizhou areas," *Xinjiang Petroleum Geology*, vol. 23, no. 2, pp. 106–110, 2002.

[23] J. Zhang, C. Wei, G. Yan, and G. Lu, "Structural and fractal characterization of adsorption pores of middle-high rank coal reservoirs in western Yunnan and eastern Guizhou: an experimental study of coals from the Panguan syncline and Laochang anticline," *Energy Exploration & Exploitation*, vol. 37, no. 1, pp. 251–272, 2019.

[24] X. L. Lai, W. Wang, P. B. Wignall, and D. P. G. Bond, "Palaeoenvironmental change during the end-Guadalupian (Permian) mass extinction in Sichuan, China," *Palaeogeography Palaeoclimatology Palaeoecology*, vol. 269, no. 1-2, pp. 78–93, 2008.

[25] H. H. Hou, L. Y. Shao, S. A. Wang et al., "Influence of depositional environment on coalbed methane accumulation in the Carboniferous-Permian coal of the Qinshui Basin, northern China," *Frontiers of Earth Science*, vol. 13, no. 3, pp. 535–550, 2019.

[26] L. Y. Shao, X. T. Wang, J. Q. Zhang et al., "CBM accumulation characteristics and exploration target selection in northeastern Yunnan, China," *Natural Gas Industry*, vol. 38, no. 9, pp. 17–27, 2018.

[27] Z. Z. Feng, "Single factor analysis and multifactor comprehensive mapping method-reconstruction of quantitative lithofacies palaeogeography," *Journal of Palaeogeography*, vol. 6, no. 1, pp. 3–19, 2004.

[28] A. H. Wang, Z. H. Wang, J. K. Liu, N. C. Xu, and H. L. Li, "The Sr/Ba ratio response to salinity in clastic sediments of the Yangtze River Delta," *Chemical Geology*, vol. 559, p. 119923, 2021.

[29] J. C. Van Wagoner, "Seismic stratigraphy interpretation using sequence stratigraphy; part 2, key definitions of sequence stratigraphy," *Atlas of Seismic Stratigraphy*, vol. 27, 1987.

[30] J. Wagoner, H. W. Posamentier, R. M. Mitchum, P. R. Vail, and J. Hardenbol, "An overview of the fundamentals of sequence stratigraphy and key definitions," in *Sea Level Changes-An Integrated Approach*, 1988.

[31] P. R. Vail, R. M. Mitchum, and S. Thompson, "Seismic stratigraphy and global changes of sea-level. In: C. E. Payton, Ed., Seismic Stratigraphy: Application to Hydrocarbon Exploration," *AAPG*, vol. 26, pp. 83–97, 1977.

[32] G. Chalmers and R. M. Bustin, "On the effects of petrographic composition on coalbed methane sorption," *International Journal of Coal Geology*, vol. 69, no. 4, pp. 288–304, 2007.

[33] M. N. Lamberson and R. M. Bustin, "Coalbed methane characteristics of Gates Formation coals, northeastern British Columbia; effect of maceral composition," *AAPG Bulletin*, vol. 77, no. 12, pp. 2032–2076, 1993.

[34] C. Guo, Y. C. Xia, D. M. Ma et al., "Geological conditions of coalbed methane accumulation in the Hancheng area, southeastern Ordos Basin, China: implications for coalbed methane high-yield potential," *Energy Exploration & Exploitation*, vol. 37, no. 3, pp. 922–944, 2019.

[35] Y. B. Yao, D. M. Liu, and T. T. Yan, "Geological and hydrogeological controls on the accumulation of coalbed methane in the

Weibei field, southeastern Ordos Basin," *International Journal of Coal Geology*, vol. 121, pp. 148–159, 2014.

[36] S. Yin and W. Ding, "Evaluation indexes of coalbed methane accumulation in the strong deformed strike-slip fault zone considering tectonics and fractures: a 3D geomechanical simulation study," *Geological Magazine*, vol. 156, no. 6, pp. 1052–1068, 2019.

[37] T. A. Moore and J. C. Shearer, "Peat/coal type and depositional environment–are they related?," *International Journal of Coal Geology*, vol. 56, no. 3-4, pp. 233–252, 2003.

[38] J. Y. Zhang, D. M. Liu, Y. D. Cai, Z. J. Pan, Y. B. Yao, and Y. J. Wang, "Geological and hydrological controls on the accumulation of coalbed methane within the No. 3 coal seam of the southern Qinshui Basin," *International Journal of Coal Geology*, vol. 182, pp. 94–111, 2017.